

The Effect of Pretreatment on Pd/C Catalysts

I. Adsorption and Absorption Properties

Nalini Krishnankutty and M. Albert Vannice

Department of Chemical Engineering, The Pennsylvania State University, University Park, Pennsylvania 16802

Received September 9, 1994; revised March 1, 1995

Pd catalysts were prepared using a high surface area carbon black which was pretreated at 1223 K under H₂ or Ar to remove sulfur contaminants and oxygen-containing functional groups on the surface. One carbon sample was oxidized by HNO₃ to create new oxygen functional groups on its surface. Pd catalysts were prepared using a Pd acetylacetonate precursor and were characterized by H₂, O₂, and CO chemisorption, hydrogen titration, X-ray diffraction (XRD) and transmission electron microscopy (TEM). Well-dispersed catalysts were indicated by the TEM and XRD results; however, chemisorption of all three gases, especially hydrogen, was substantially suppressed on all catalysts. XRD patterns indicated an expansion of the Pd lattice in these catalysts, which is attributed to the presence of carbon atoms within the Pd lattice. This expansion was accompanied by a decreased ability to form the β -phase hydride compared to bulk Pd and Pd dispersed on oxide supports. However, heats of adsorption for H₂, O₂, and CO on these catalysts were reasonably consistent with previously reported values. The suppressed chemisorption and hydride formation is attributed to carbon contamination of the Pd although sulfur contamination of the Pd on the untreated carbon support also occurred. The ability to form hydrides was partially regained after mild O₂ cleaning procedures, but only a limited enhancement in chemisorption was observed. Reduction at 673 K gave normal Pd β -hydride ratios, but chemisorption was still suppressed. © 1995 Academic Press, Inc.

INTRODUCTION

Carbon-supported metals are used industrially for both the small-volume manufacturing of organic fine chemicals and the high-volume production of intermediates like polyurethane, polyesters, and nylon (1–4). Carbon supports have high surface area, are inexpensive, are inert in corrosive environments, and precious metals supported on them can be easily recovered. Further, their pore structure and surface area can be varied relatively easily. However, commercial carbon-supported metal catalysts can sometimes exhibit large batch-to-batch variations in performance

which can be due, at least partially, to natural variations in the starting materials (3–5), and few studies have dealt with systematic variations of carbon properties in relation to catalyst performance (6).

The present study was aimed at studying the effect of carbon pretreatment prior to impregnation on the preparation and performance of Pd/C catalysts. A high surface area carbon black was pretreated at 1223 K to remove reactive S impurities and oxygen-containing functional groups from the carbon surface. Pd was chosen as the dispersed metal because it is widely used in industrial hydrogenation reactions (2); also, Pd/C catalysts have been reported to exhibit significant variations in catalytic performance and have lower specific activity compared to Pd on other supports for reactions like benzene and 1,3 butadiene hydrogenation (7–9). Our initial results showed that pretreatment of the carbon support did not alter the Pd dispersion in our catalysts, but unexpected adsorption and catalytic behavior was observed; consequently, the effect of catalyst pretreatment on the behavior of carbon-supported Pd was emphasized. These Pd/C catalysts were characterized by TEM and XRD, by chemisorption of H₂, O₂, and CO, by heats of adsorption, and by their ability to form the Pd β -hydride phase. The catalytic properties of these catalysts are described in the following paper (10).

EXPERIMENTAL

Pretreatments of Carbon

Black Pearls 2000 (BP2000, Cabot Corp.), referred to as C-AS IS, is a carbon black with a specified surface area of 1475 m²/g, 0.36% ash, and 1.3 wt% S. It was given different pretreatments in order to change the chemical nature of the carbon surface (11). A high temperature treatment (HTT) under flowing H₂ or Ar (75 sccm) for 16 h at 1223 K decreased the S content to $\leq 0.1\%$ and removed oxygen from the carbon surface (12); these samples were labelled C-HTT-H₂ and C-HTT-Ar, respectively. The

former had chemisorbed hydrogen on its surface (11, 13). These supports were transferred without air exposure to a N₂-purged glove box and stored. The C-HNO₃ sample was prepared by boiling a C-HTT-Ar sample in 15.8 *N* HNO₃ for 6 h. After repeated aqueous washes and filtration, the C-HNO₃ was dried overnight. Further details regarding the pretreatments of the carbon support can be found elsewhere (11).

Preparation of Pd/C Catalysts

An anaerobic incipient wetness method was used to prepare approximately 3 wt% Pd/C catalysts utilizing standard Schlenk techniques (14). Palladium acetylacetonate, Pd(C₅H₇O₂)₂ (99%, Aldrich Chem. Co.), dissolved in dried, degassed tetrahydrofuran (THF) was used as the precursor to produce Cl-free catalysts. The catalysts were evacuated overnight at 300 K, then at 353 K for 2 h to remove any THF, and transferred anaerobically to a N₂-purged glove box; further transfers to chemisorption and reaction cells were done here. Two Pd/C catalysts were also prepared using C-HTT-H₂ as support and PdCl₂ dissolved in water. Other catalysts studied for comparison were 0.48% Pd/SiO₂ and 1.45% Pd/Grafoil made from Pd(NH₃)₄(NO₃)₂ (15, 16), and commercial 3.61% Pd/C and 5% Pd/Al₂O₃ catalysts (Johnson Matthey). A 99.999% Pd powder (Johnson Matthey) was used after cleaning in a flow of 20% O₂ and 80% He at 773 K for 30 min, followed by a 1 h reduction at 573 K in a flow of 20% H₂ and 80% He. Further details regarding catalyst preparation are given elsewhere (20).

Characterization of Pd/C Catalysts

Volumetric adsorption measurements were made in stainless steel systems giving a dynamic vacuum <10⁻⁶ Torr at the sample location (17). H₂, He, and O₂ (99.999% purity, MG Ind.) and CO (99.99%, Matheson) were purified by flowing them through drying tubes (Supelco), and He and H₂ were also passed through Oxytraps (Alltech Assoc.). Approximately 0.1–0.2 g of a catalyst was heated to 393 K in 50 sccm He and held at 393 K for 1 h before being heated in He to either 573 or 673 K, reduced in 50 sccm H₂ for 2 h, then evacuated at the reduction temperature for 1 h and cooled under vacuum to the chemisorption temperature (15). Reduction at 573 K has been reported to give the best dispersions (18), and Pd may not be completely reduced below 573 K (19). Longer reduction and evacuation times had no effect on the chemisorption uptakes and hydride formation (20). The effect of pretreatment in 2% O₂, over the temperature range 473–623 K and over time, on the chemisorption behavior was studied for the Pd/C-AS IS catalyst, and the optimum procedure of heating at 573 K for 30 min followed by a 2 h reduction in H₂ at 573 K was used for the catalysts discussed here (20). The gases evolved during this O₂ pretreatment were

monitored on-line by a UTI mass spectrometer. Isotherms for H₂, O₂, and CO were measured at 300 K; the method of Benson *et al.* was used for determining irreversible and reversible hydrogen uptakes and hydride ratios (21), the dual isotherm technique of Yates and Sinfelt was used for CO uptakes (22), and a dual isotherm method using a 30 min evacuation between isotherms was used for O₂ uptakes.

Ex situ XRD measurements were made on samples previously used for chemisorption using a Rigaku Geigerflex diffractometer equipped with a CuK α radiation source and a graphite monochromator. Metal crystallite sizes, *d*, were calculated from the line width of the Pd(111) peak using the Scherrer equation with Warren's correction for instrumental line broadening, i.e., $d = K\lambda / \{\beta^2 - B^2\}^{1/2} \cos \theta$, where $K = 0.9$ and $B = 0.22$ at a 2θ value of 40.2°. Samples after chemisorption were observed in a Philips 420T transmission electron microscope at a high tension voltage of 120 kV. The samples were dispersed in acetone ultrasonically and placed on a 400-mesh, carbon-coated copper grid. Pd particle size distributions were obtained by counting 500–1500 Pd particles for each catalyst.

Energy changes during chemisorption of H₂, O₂, or CO and during bulk β -hydride formation at 300 K were determined on a modified Perkin-Elmer DSC-2C differential scanning calorimeter (23). Approximately 3.5 mg of catalyst was given the same pretreatment as that used prior to chemisorption, except that 40 sccm of 20% H₂/80% Ar was used and adsorbed H₂ was removed by purging the sample with 45 sccm of an Ar/He mixture (77% Ar) for 1 h at 573 K. As with the chemisorption measurements, two exposures were made with each gas, thus allowing isothermal, integral heats of irreversible and reversible adsorption or hydride formation to be determined (20).

RESULTS

Pd Particle Size Distribution

A typical TEM micrograph is shown in Fig. 1 for a representative Pd/C-HTT-Ar sample after reduction at 573 K, and the corresponding Pd particle size distribution is shown in Fig. 2. The number-average diameter, $d_n = \sum n_i d_i / \sum n_i$, surface-area-weighted average diameter, $d_s = \sum n_i d_i^3 / \sum n_i d_i^2$, and volume-weighted average diameter, $d_v = \sum n_i d_i^4 / \sum n_i d_i^3$, of the Pd particles in the catalysts are presented in Table 1; further details are presented elsewhere (20). Fairly narrow Pd particle size distributions were obtained for all catalysts made from Pd(AcAc)₂ after a 573 K reduction, irrespective of carbon pretreatment—Pd/C-AS IS, Pd/C-HTT-H₂, and Pd/C-HTT-Ar have similar number-average Pd particle sizes, 3.5–4.3 nm, but Pd/C-HNO₃ has a slightly larger size, 6.3 nm. This small increase may be due to the lower surface area of the C-HNO₃ support (11) and shows that small Pd

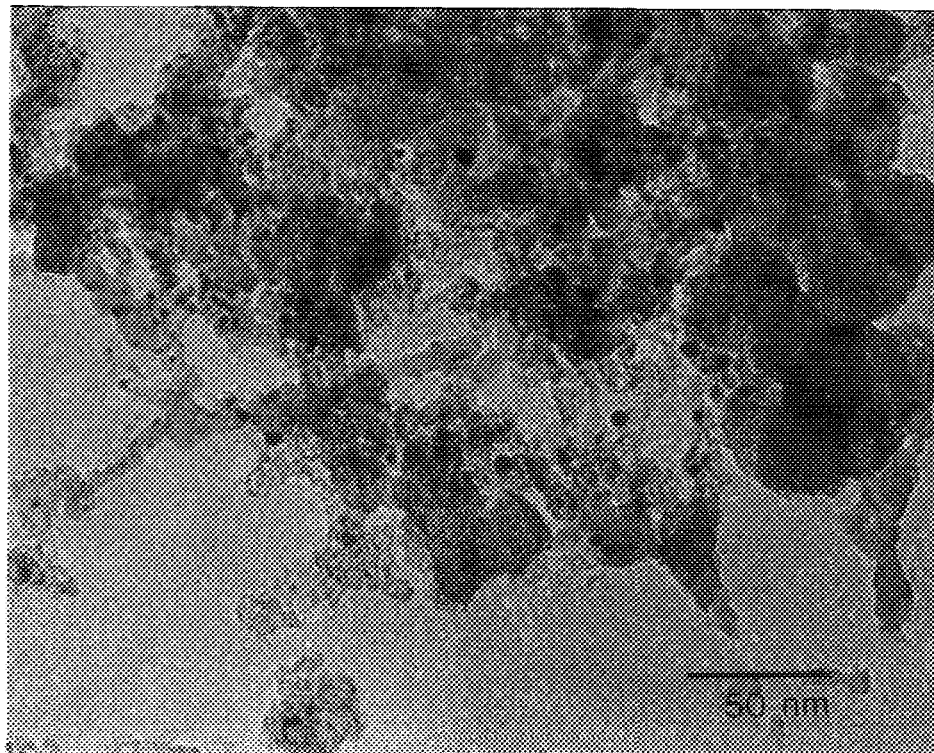


FIG. 1. TEM micrograph of Pd/C-HTT-Ar after a 573 K reduction.

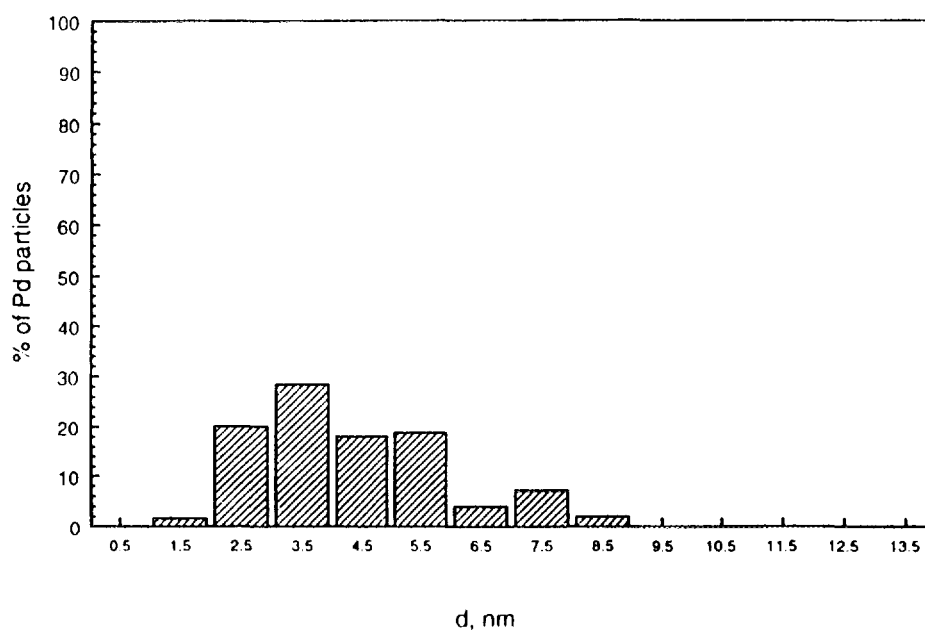


FIG. 2. TEM particle size distribution of Pd particles in 3.1% Pd/C-HTT-Ar after a reduction at 573 K (Based on 800 particles).

TABLE 1
Comparison of Average Pd Particle Sizes from TEM^a

Catalyst	T_{red} (K)	d_n (nm)	d_s (nm)	d_v (nm)	Dispersion based on d_s
2.6% Pd/C-AS IS	573 K	3.5	4.0	4.2	0.28
2.8% Pd/C-HTT-H ₂	573 K	4.0	4.8	5.3	0.24
3.1% Pd/C-HTT-Ar	573 K	4.3	5.6	6.2	0.20
2.3% Pd/C-HNO ₃	573 K	6.3	7.2	7.7	0.16
2.1% Pd/C	573 K	3.3	20.7	33.0	0.05
3.4% Pd/C	573 K	3.5	7.4	10.5	0.15
3% Pd/C-AS IS	573 K	4.3	9.6	15.1	0.12
3% Pd/C-AS IS ^b	573 K	3.6	6.5	8.1	0.17
2.1% Pd/C	673 K	7.0	10.6	11.6	0.11
2.6% Pd/C-AS IS	673 K	7.5	22.7	29.6	0.05

^a Number average (d_n) surface-area-weighted average (d_s), and volume-weighted average (d_v) particle sizes.

^b Heated in 2% O₂ for 30 min at 573 K before reduction in H₂ at 573 K.

particles were not preferentially stabilized by the oxygen groups on the surface of C-HNO₃. This result differs from that reported by Suh *et al.*, in which oxygen groups increased Pd dispersion on carbon; however, a different Pd precursor was used (7). O₂ pretreatment of a Pd/C catalyst prior to reduction decreased the average size of Pd particles, in accordance with previously reported results (24).

Broader distributions were obtained with the PdCl₂ precursor and large particles of Pd up to 45 nm were observed (20). This is consistent with the sintering of Pd particles from PdCl₂ at higher temperatures (25, 26), but the unusually large Pd particles may also be due to beam damage or problems associated with passivation. Difficulties related to passivation are suggested because the 2.1% Pd/C catalyst had some 50 nm particles after a 573 K reduction while the largest size after a 673 K reduction was 17 nm. All TEM samples of Pd/C catalysts made from Pd(AcAc)₂ were passivated by CO chemisorbed on the Pd surface before air exposure, whereas the 2.1% Pd/C and 3.4% Pd/C samples were not similarly passivated and had chemisorbed hydrogen present when exposed to air (20). The coalescence of nonpassivated Pd particles upon exposure to oxygen and further electron-beam-induced coalescence of these particles has been observed previously (27). Higher reduction temperatures induced sintering, as seen for the Pd/C-AS IS and 2.1% Pd/C samples reduced at 673 K, in accordance with previously reported behavior (19).

X-Ray Diffraction

A broad Pd(111) peak, shifted from 40.11° to lower angles, was seen in the XRD patterns of most of the Pd/C catalysts after reduction at 573 K, as shown in Fig. 3A. The peaks corresponding to the amorphous carbon are

analyzed elsewhere (11). The Pd(111) peak positions for the various Pd catalysts and the corresponding lattice parameters are given in Table 2. Catalysts made from PdCl₂ had peak positions closer to the Pd(111) position of 40.11°. The shift of the Pd(111) peak to lower angles indicates a lattice expansion, attributed to interstitial C atoms. For samples exposed to H₂ at 673 K or above, the Pd peak was close to 40.11° and the lattice parameter was near the value of 3.889 Å for bulk Pd. The Pd peak was between 39° and 40° after O₂ pretreatment, indicating a lattice parameter of 3.92–3.95 Å. Figure 3B shows the shift of the Pd(111) peak in the Pd/C-HNO₃ sample at different reduction temperatures.

Chemisorption

The importance of an appropriate cleaning procedure is demonstrated by the adsorption behavior of H₂ on the 99.999% Pd powder, as shown in Fig. 4. No irreversible uptake was detected after a reduction in H₂ at 573 K, indicating Pd surface contamination. However, following a 30-min cleaning procedure in 20% O₂ and 80% He at 773 K prior to reduction in H₂ at 573 K, irreversible H₂ uptake occurred. The number of surface Pd atoms/g Pd (1.2×10^{19}) obtained using the accepted stoichiometry of 1 H_{ad}:1 Pd_s at 300 K was consistent with the Ar BET surface area of 0.837 m²/g Pd (i.e., 1.0×10^{19} surface Pd atoms/g Pd). A normal hydride ratio of 0.64 was obtained after this pretreatment (20).

Typical isotherms for H₂ adsorption and absorption on Pd/C catalysts are shown in Fig. 5, and the corresponding uptakes are reported in Table 3. Figure 5 shows that the slopes of the H₂ isotherms are dependent on the carbon pretreatment and that a sharp transition near ~14 Torr due to the formation of the Pd β-hydride phase does not necessarily occur (28). The transition is gradual and occurs over a pressure range up to 60 Torr for Pd supported on the HTT carbons. The shapes of the H₂ isotherms obtained for these Pd/C catalysts are consistent with the isotherms for a Pd/SiO₂ catalyst after carburization with a C₂H₂ + H₂ mixture (29); however, it has been suggested that this gradual transition is due to a distribution of Pd particle sizes in the catalyst (30). The Pd/C-AS IS sample with a similar particle size distribution did not show the typical low-pressure rise due to hydride formation in its H₂ isotherm and sometimes gave uptakes resulting in no irreversible hydrogen chemisorption (20); this behavior is attributed to sulfur initially present in the C-AS IS which migrated onto the Pd surface. The H₂ uptakes on the Pd catalysts prepared from PdCl₂ showed the large transition to β-hydride formation at lower pressures (20); however, the 3.4% Pd/C-HTT-H₂ had a significantly lower hydride ratio than the normal bulk value near 0.66 (28).

Using accepted 1:1 adsorption stoichiometries for

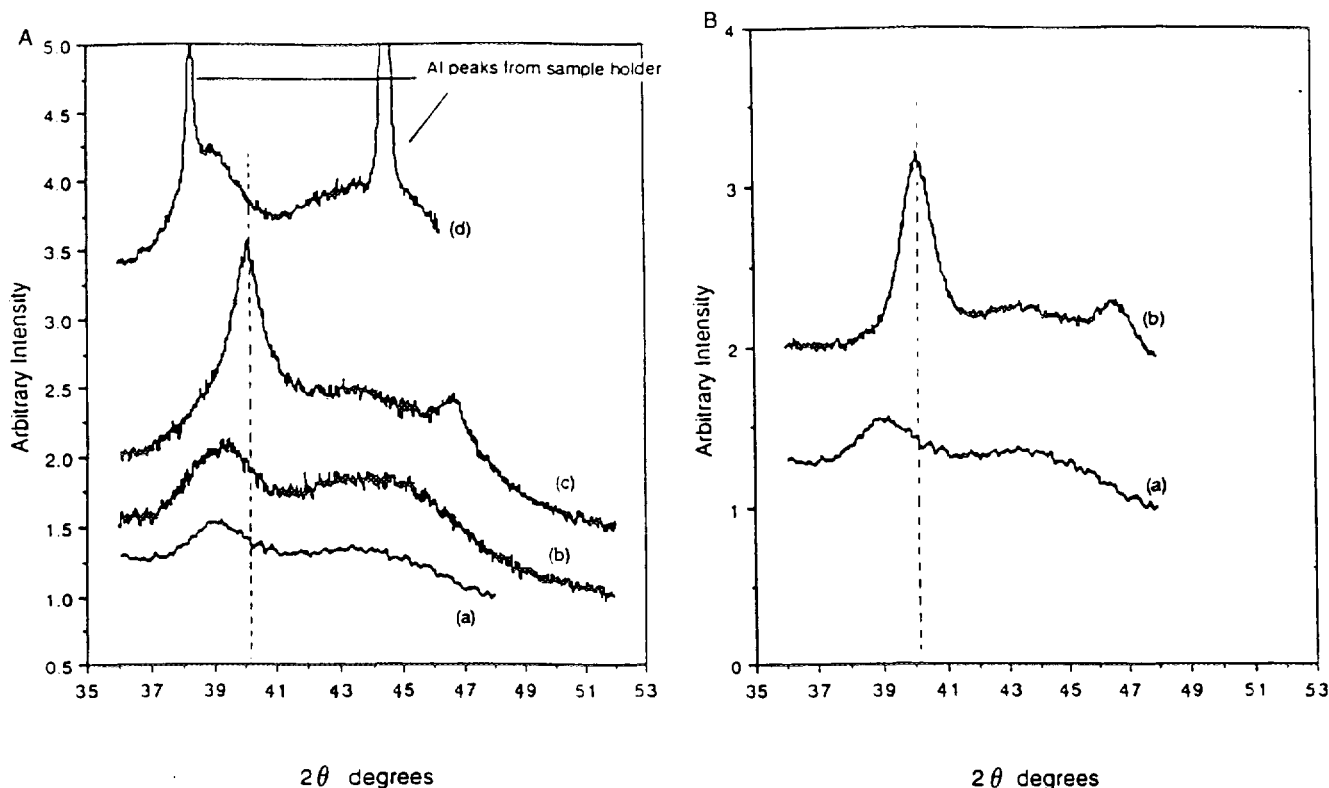


FIG. 3. (A) Comparison of XRD patterns obtained for Pd/C catalysts after 573 K reduction: (a) 2.3% Pd/C-HNO₃, (b) 2.6% Pd/C-AS IS, (c) 3.4% Pd/C-HTT-H₂, and (d) 3.1% Pd/C-HTT-Ar. (B) Comparison of XRD patterns obtained for Pd/C-HNO₃ after (a) 573 K reduction and (b) CO hydrogenation at 673 K.

$H_{ad}:Pd_s$, $O_{ad}:Pd_s$, and $CO_{ad}:Pd_s$, where Pd_s represents a surface Pd atom (21, 31, 32), Pd dispersions were calculated from the irreversible gas uptakes and are presented in Table 3. For a given sample, these dispersions do not agree well, in contrast to the behavior of Pd on oxide supports like SiO₂, Al₂O₃, SiO₂-Al₂O₃, and rare earth oxides (15, 21, 31, 33), and H/Pd ratios were typically the lowest while CO/Pd ratios were the highest. The high O₂ uptake on 2.3% Pd/C-HNO₃ is due to a high irreversible uptake on the C-HNO₃ support (11). For a commercial 3.61% Pd/C catalyst, the dispersion from H₂ chemisorption was consistent with the 8.9 nm particle size from XRD, but the dispersion from O₂ chemisorption was almost 5 times higher. This is most likely due to promoters (mostly Na and Ca) in this catalyst but could also be due to adsorption on the carbon since all the adsorbed oxygen could not be titrated (20). For the 2.1% Pd/C and 3.4% Pd/C catalysts made from PdCl₂, the irreversible O₂ and CO uptakes were consistent with each other, but were 2–3 times higher than the H₂ uptakes. The results in Tables 1 and 3 indicate a substantial suppression of chemisorption for all three gases, with CO chemisorption typically giving dispersions closest to those from TEM. It must be noted that pretreatment of the

carbon support can complicate isotherms by inducing irreversible O₂ adsorption on the carbon support.

Palladium forms two bulk hydride phases, α and β , and at 300 K the maximum H_{ab}/Pd_{bulk} ratio for bulk Pd is ~ 0.66 (28), but this can vary with the extent of alloying in Pd alloys (34). The β -hydride ratio does not appear to be influenced by particle size if particles are larger than 1.5 nm (35–37), but it can be reduced to zero as dispersion approaches unity and bulk Pd atoms disappear. After reduction at 573 K, all the Pd/C catalysts except 2.1% Pd/C had low bulk hydride ratios of 0.2–0.35. The hydride ratios did not change after longer evacuation times at 573 K during catalyst pretreatment, at 298 K between isotherms, or at 273 K (20), which is consistent with the behavior reported for carburized Pd/SiO₂ catalysts (29). The commercial Pd/C catalyst, the Pd/Grafoil catalyst, the commercial 5% Pd/Al₂O₃ catalyst, and the UHP Pd powder yielded reasonable hydride ratios of 0.53 to 0.64, while the apparent hydride ratio of 0.85 for 0.48% Pd/SiO₂ is due to increased reversible H₂ chemisorption on very small Pd crystallites (15, 31).

Either exposure to reducing conditions at 673 K and above or use of an O₂ pretreatment prior to reduction at

TABLE 2
Pd XRD Peak Positions, Lattice Constants, and Crystallite
Sizes for Pd/C Catalysts

Catalyst	T_{red} (K)	Pd (111) peak position (2θ)	Pd (200) peak position (2θ)	Pd lattice constant a , (Å)	d_{XRD}^a (nm)	Hydride ratio (H_{ad}/Pd_b)
2.6% Pd/C-AS IS	573	39.41	—	3.961	4.0	0.28
2.8% Pd/C-HTT-H ₂	573	—	—	—	—	0.21
3.1% Pd/C-HTT-Ar	573	39.23	—	3.978	—	0.23
2.3% Pd/C-HNO ₃	573	39.08	—	3.990	4.7	0.35
2.1% Pd/C	573	40.10	—	3.894	27.9	0.68
3.4% Pd/C	573	40.12	46.61	3.893	5.7	0.36
3% Pd/C-AS IS	573	—	—	—	—	0.005
3% Pd/C-AS IS ^b	573	39.82	—	3.921	5.0	0.21
2.8% Pd/C-HTT-H ₂ ^b	573	39.52	—	3.950	3.5	0.38
2.3% Pd/C-HNO ₃ ^b	573	—	—	—	—	0.42
2.6% Pd/C-AS IS	673	—	—	—	—	0.40
2.8% Pd/C-HTT-H ₂ ^c	573	39.81	46.40	3.922	7.2	0.51
2.3% Pd/C-HNO ₃ ^c	573	40.17	46.58	3.888	7.2	0.64
2.1% Pd/C	673	39.80	46.32	3.924	11.8	0.77
Pd (JCPDS card No. 5-681)	—	40.115	46.662	3.890	—	—

^a From Scherrer equation.

^b Heated in 2% O₂, 98% He for 30 min at 573 K before reduction.

^c Used for CO hydrogenation above 723 K (Ref. (10)).

573 K were found to affect hydride ratios and uptakes, as shown in Table 4. These results show that higher reduction temperatures increased bulk hydride formation, and nearly normal hydride formation was obtained after a 673 K reduction but chemisorption was still suppressed. However, after an O₂ pretreatment, H₂ and O₂ chemisorption and hydride formation typically increased, while CO uptakes either increased or remained unchanged. During the O₂ pretreatment, CO and CO₂ evolution from the HTT carbon catalysts was detected by mass spectrometry, and evolution of SO₂ was also detected from the Pd/C-AS IS sample (20).

Heats of Adsorption

Isothermal, integral heats of adsorption of H₂, O₂, and CO on these Pd surfaces were obtained in order to probe adsorption states and determine if weaker binding was associated with the suppressed chemisorption; these values are presented in Table 5. Q_{ad} values for irreversible hydrogen adsorption on these Pd/C catalysts range from 16 to 24 kcal/mole, consistent with previous results for C-supported Pd which ranged between 21 and 25 kcal/mole for crystallites larger than 4 nm (38, 39), while they are slightly higher than the integral Q_{ad} values of 15 ± 1 kcal/mole determined for Pd crystallites larger than 3 nm on other supports (15). Initial Q_{ad} values at low H coverage have varied from 20 to 27 kcal/mole (40–48). The Q_{ad} values for irreversible oxygen adsorption on Pd supported on the S-free carbons

varied between 45 and 55 kcal/mole, which is within the range found for Pd crystallites larger than 3 nm (average integral value of 50 kcal/mole) (49); while Q_{ad} values for O₂ on Pd films and single crystals have ranged from 55 to 80 kcal/mole O₂ (50). However, the sulfur-containing Pd/C-AC IS sample gave an unusually low Q_{ad} value of 35 kcal/mole for O₂. The Q_{ad} values of 17 to 21 kcal/mole for CO on these Pd/C catalysts are lower than initial heats of adsorption on clean Pd surfaces, i.e., 32–40 kcal/mole on Pd (48, 50, 51), as well as isothermal, integral Q_{ad} values of 23 ± 3 kcal/mole for supported Pd crystallites larger than 3 nm (52). However, in a recent TPD study, Stará *et al.* observed two CO species with desorption energies of 22 and 29 kcal/mole from clean Pd particles supported on Al₂O₃, whereas CO adsorption on a carbon-covered Pd surface occurred primarily on lower energy sites with a desorption energy of 23 kcal/mole (53). In addition, Q_{ad} for CO on the higher energy sites was lowered on the carbon-covered Pd surface, which resulted in an additional decrease in the overall heat of CO adsorption (53).

The exotherms associated with reversible H₂ uptakes on Pd/C catalysts should provide values close to the heats of β -phase hydride formation reported for both bulk Pd and supported Pd, and the apparent heats of β -hydride formation, assuming all the reversible H₂ uptake is associated with this phase, are also given in Table 5. All values are within the range of 9 ± 1 kcal/mole established by numer-

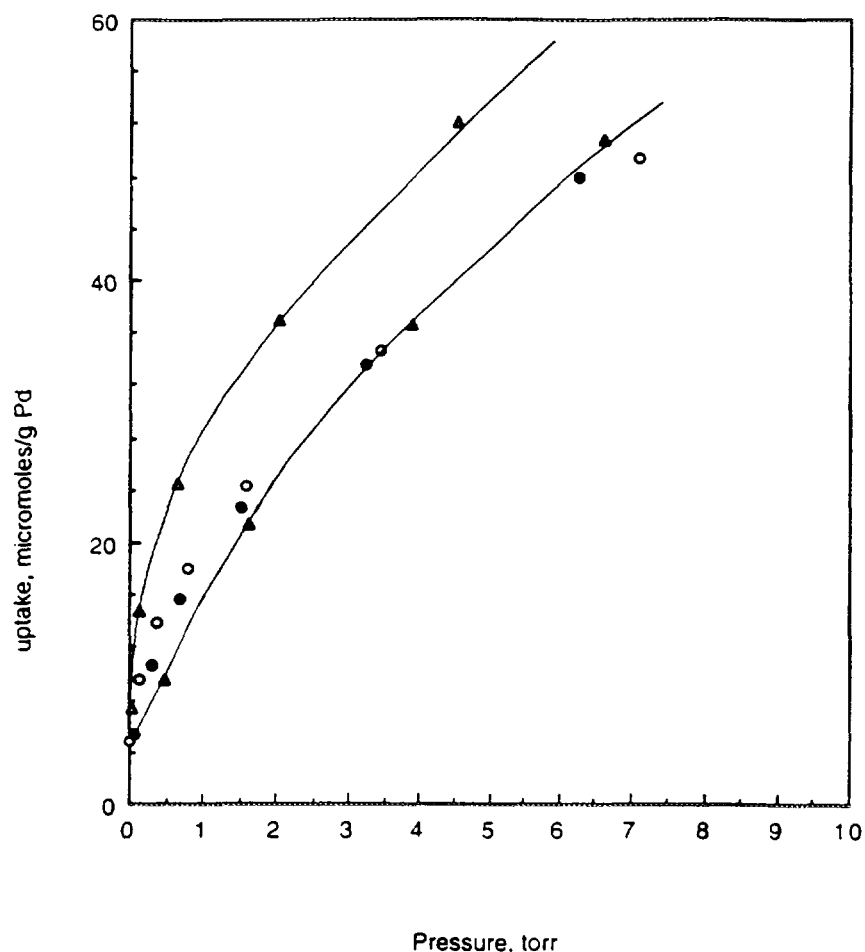


FIG. 4. H_2 uptake at 300 K on Pd powder (99.999%) with (Δ , \blacktriangle) and without (\circ , \bullet) 30 min cleaning in O_2 at 773 K prior to 2 h reduction at 573 K. Open symbols indicate first isotherm and closed symbols indicate second isotherm.

ous studies over a 35-year period (15, 38, 47, 54–60); only the result for one sintered Pd black sample examined by Artamonov *et al.* (61) and the results reported by Phillips and co-workers (16) have deviated from this range. One explanation for this latter discrepancy is contamination; for example, Pd (and Pt) black samples can have significant amounts of alkali metal impurities (62), and the presence of K on Pd can decrease the coverage of adsorbed hydrogen but increase the binding energy (63). The sintering step employed by the Russian workers (61) would concentrate the contaminants on the Pd surface. The inconsistency of the results of Wunder *et al.* (16), attributable also to contamination, is discussed in much greater detail elsewhere (20).

DISCUSSION

Carbon is often considered to be an inert support, but its affinity for O_2 and the possibility of hydrogen spillover can complicate the measurement of metal dispersions by

O_2 and H_2 adsorption, H_2 TPD, and H_2 titration (3, 7, 9). H_2 chemisorption at 343 K gave dispersions consistent with those from TEM for Pd supported on a high purity Vulcan black after a 673 K reduction (24), and Ryndin *et al.* reported good agreement between particle sizes from TEM and H_2 titration at 298 K for Pd supported on a graphitic carbon although it is not clear if a correction was made for hydride formation (19). However, two desorption peaks around 383 and 593 K, associated with hydrogen on Pd and on carbon, respectively, were observed by Ouchaib *et al.* during H_2 TPD from a Pd/activated carbon sample, and Pd dispersion calculated from only the low temperature peak agreed with dispersions from TEM (9). Conventional H_2 adsorption at 298 K would have given artificially high dispersions for the above Pd/C catalyst due to the irreversible hydrogen uptake on the carbon. Konvalinka and Scholten found reasonable agreement between Pd particle sizes from CO chemisorption and those from TEM for Pd/activated carbon (38), and Suh *et al.* found that pulsed O_2 titration of adsorbed hydrogen at 298 K gave Pd disper-

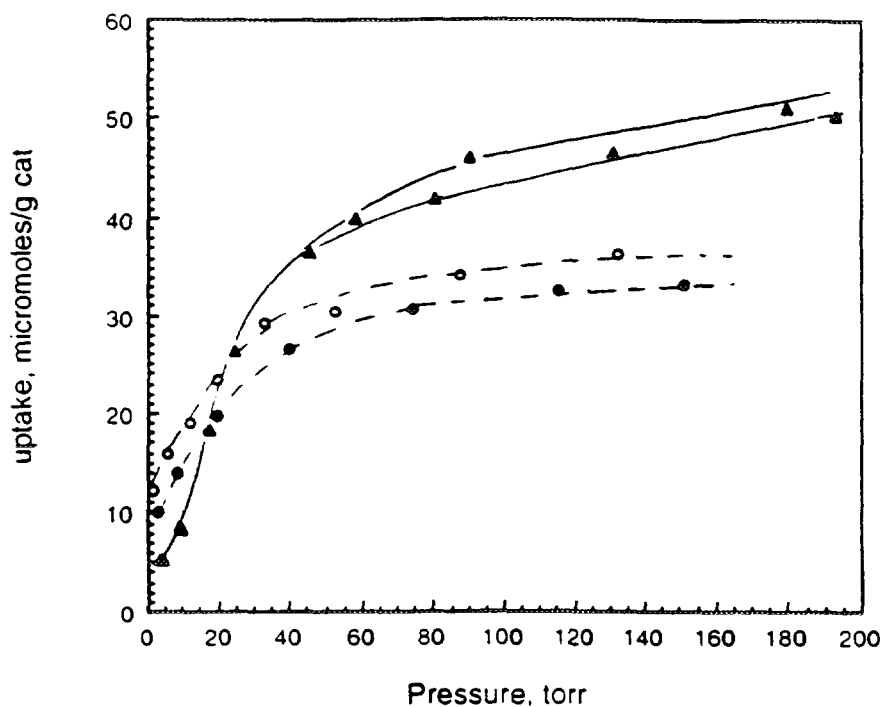


FIG. 5. H_2 uptakes at 300 K on Pd/C catalysts made from $Pd(AcAc)_2$ after 2 h reduction at 573 K. Open symbols indicate first isotherm and closed symbols indicate second isotherm: (○, ●) 2.8% Pd/C-HTT- H_2 , (△, ▲) 2.3% Pd/C- HNO_3 .

sions consistent with TEM; however, H_2 titration uptakes at 373 K were high compared to the number of surface Pd atoms, indicating H_2 spillover may have occurred (7). These carbons had not been cleaned by a HTT prior to use. Thus, although chemisorption of different gases has

been used previously to characterize Pd/C catalysts, their behavior has varied significantly and a thorough comparison of H_2 , O_2 , and CO adsorption on well-characterized Pd dispersed on a clean carbon is lacking. In addition, almost no information exists on the hydride-forming ability

TABLE 3

Gas Uptakes, Apparent Pd Dispersions, and Bulk Hydride Ratios, $T_{red} = 573$ K

Catalyst	Irreversible uptake ($\mu\text{mole/g cat}$)			Apparent dispersion			H_{rev}/Pd_b	
	H_2	O_2	CO	H_{irr}/Pd_t	O_{ad}/Pd_t	CO_{ad}/Pd_t	^a	^b
2.6% Pd/C-AS IS	7	6	—	0.06	0.05	—	0.28	0.37
2.8% Pd/C-HTT- H_2	4	8	35	0.03	0.06	0.13	0.21	0.27
3.1% Pd/C-HTT-Ar	6	8	27	0.04	0.05	0.09	0.23	0.25
2.3% Pd/C- HNO_3	2	32	6	0.02	0.19 ^c	0.03	0.35	0.41
2.1% Pd/C	16	36	75	0.16	0.36	0.38	0.63	0.56
3.4% Pd/C	20	56	112	0.13	0.35	0.35	0.36	0.37
1.45% Pd/Grafoil	8	8	—	0.12	0.12	—	0.53	—
3.61% Pd/C-comm	30	146	101	0.18	0.62	0.25	0.59	—
0.48% Pd/ SiO_2	12	12	—	0.53	0.53	—	0.85	—
5% Pd/ Al_2O_3 -comm	57	—	—	0.24	—	—	0.56	0.56
99.999% Pd powder	10	—	—	0.002	—	—	0.64	—

^a Based on dispersions from H_2 chemisorption.

^b Based on dispersion from TEM.

^c Corrected for irreversible uptake on support (Ref. (11)).

TABLE 4
Effect of Pretreatment on H₂, O₂ and CO Adsorption on Pd/C Catalysts

Catalyst	T _{red} (K)	Irreversible gas uptakes (μmole/g cat)			d _s ^a (nm), based on			d _s ^b (nm)	d _v ^c (nm)	(H _{ab} /Pd _b)
		H ₂	O ₂	CO	H _{ad}	O _{ad}	CO _{ad}			
3% Pd/C-AS IS	573	1.9	7	28	87	23	11	9.6	—	0.005
3% Pd/C-AS IS ^d	573	3	10	16	54	16	20	6.5	—	0.21
2.6% Pd/C-AS IS	573	7	6	—	19	23	—	4.0	4.0	0.28
2.6% Pd/C-AS IS	673	5	20	—	28	7.1	—	22.7	—	0.4
2.8% Pd/C-HTT-H ₂	573	4	8	35	38	19	8.7	4.8	—	0.21
2.8% Pd/C-HTT-H ₂ ^d	573	4	4	29	38	38	10	—	7.1	0.47
2.8% Pd/C-HTT-H ₂ ^e	573	14	16	35	10	9.4	8.8	—	3.5	0.38
2.3% Pd/C-HNO ₃	573	2	21 ^f	6	57	3.9	38	7.2	4.4	0.35
2.3% Pd/C-HNO ₃ ^d	573	2	28 ^f	8	57	3.2	31	—	7.2	0.64
2.3% Pd/C-HNO ₃ ^e	573	4	21 ^f	13	28	3.9	19	—	—	0.42

^a Calculated using $d = 1.13/\text{dispersion}$.

^b From TEM.

^c From XRD.

^d Used for CO hydrogenation above 673 K (Ref. (10)).

^e Heated in 2% O₂ for 30 min at 573 K before reduction.

^f Corrected for adsorption on support (Ref. 11)).

of C-supported Pd. Furthermore, in previous studies of Pd/C catalysts, the catalysts were always exposed to air and impurities in the carbon supports were seldom considered or reported.

The carbon black in this study had only ppm metallic impurities (11), reactive S was removed by the HTT step, oxygen-containing functional groups were eliminated to obtain clean carbon surfaces, and neither the carbon nor the catalysts were subsequently exposed to air. The Pd/C catalysts in this study were fairly well dispersed, as indicated by the 3–5 nm particle sizes from TEM and XRD,

but the chemisorption of all gases at 300 K was suppressed on these catalysts after a 573 K reduction. Further, the dispersions calculated from H₂, O₂, and CO chemisorption were not consistent, as indicated in Table 3, which is at variance with the good agreement typically obtained from H₂, O₂, and CO chemisorption on Pd supported on oxides (15, 31, 33, 49, 52). In addition, these Pd/C catalysts showed a decreased ability to form the β-hydride phase after reduction at 573 K, except for the rather poorly dispersed 2.1% Pd/C and Pd/Grafoil samples, as shown in Table 3. The suppressed chemisorption and hydride formation in the

TABLE 5
Heats of Irreversible H₂, O₂, and CO Chemisorption on Pd and Pd β-phase Hydride Formation with Pd/C Catalysts at 300 K, T_{red} = 573 K

Catalyst	Q _{ads} (kcal/mole H ₂)	Q _{abs} (kcal/mole H ₂)	Q _{ads} (kcal/mole O ₂)	Q _{ads} (kcal/mole CO)
2.6% Pd/C-AS IS	—	9.9 ± 0.6	35.0	18.9
2.8% Pd/C-HTT-H ₂	23.9 ± 2.5	12.7 ± 1.7	55.7	17.1
3.1% Pd/C-HTT-Ar	16.0 ± 0.3	12.4 ± 1.6	53.9	17.2
2.3% Pd/C-HNO ₃	21.7 ± 1.7	9.9 ± 0.2	44.8 ^b	20.9
2.1% Pd/C	18.9	10.7	—	20.4
0.48% Pd/SiO ₂ ^a	17 ^a	9.5 ^a	—	30.0
99.999% Pd powder	14.9 ^a	8.4, 9.1 ^a	53 ^c	24 ^d

^a From Ref. (15).

^b Corrected for values on carbon support (Ref. (11)).

^c From Ref. (49).

^d From Ref. (52).

Pd/C catalysts were accompanied by slightly higher heats of H₂ adsorption and hydride formation compared to Pd/oxide supports, while Q_{ad} values for CO were lower, and those for O₂ were similar to previous values (15, 38, 49, 50, 52). The effect of sulfur on Pd is not known, but preadsorbed S on Pt decreases the irreversible H₂ uptake and Q_{ad} by 15–28% as well as the initial binding energy of CO on Pt(111) and Pt(110) surfaces (64). If Pd exhibits similar behavior, this can account for the low Q_{ad} values and suppressed H₂ adsorption on Pd/C-AS IS.

These results verify that anomalous chemisorption behavior of carbon-supported Pd can occur. The low H₂ uptakes are unusual because it is well established that clean Pd adsorbs as well as absorbs H₂ at 300 K (15, 28, 40), and decreases in the magnetic susceptibility of Pd due to these separate processes have been reported earlier (65). Although a decrease in hydride formation with increasing dispersion has been suggested previously (35, 36), the low hydride values found in this study are not due to a particle size effect because Pd particles that were 3–5 nm and smaller have exhibited bulk hydride ratios near 0.6 when supported on various oxides (15, 31, 33, 37). However, Pd alloys can exhibit suppressed hydride formation (34), and contaminants like Zn, Pb, and Ca, as well as C, have been reported to suppress β -hydride formation completely and to decrease the amount of weakly adsorbed H₂ that is associated with the formation of absorbed hydrogen (38, 66). This unusual chemisorption and hydride formation behavior of Pd dispersed on high surface area turbostratic carbon is now discussed in more detail.

The most obvious explanation for the adsorption behavior exhibited by these Pd/C catalysts employing a clean turbostratic carbon support is the following: During the typical pretreatment used in this study, C atoms occupy both surface and bulk interstitial Pd sites. Some of this could occur during decomposition of the Pd(AcAc)₂ precursor. Additional surface contamination can occur when significant amounts of sulfur are present in the carbon support, as verified by SO₂ evolution during cleaning of the Pd/C-AS IS sample in O₂. However, with the HTT carbon supports, no S-containing gases were observed during catalyst regeneration in O₂, and the lower adsorption capacities must be attributed to carbon contamination (20). The decrease in the Pd lattice parameter after an O₂ treatment, as noted in Table 2, and the increase in H₂ and O₂ chemisorption and hydride ratios, as shown in Table 4, also indicate that carbon is removed from the Pd particles during the treatment in O₂. The sharp decrease in CO and CO₂ evolution with time further implies that their formation is associated primarily with the Pd, rather than the support, because gasification of the latter would give a constant rate (20).

Although it has been commonly accepted that the second- and third-row Group VIII metals do not form bulk

interstitial carbides (67), the existence of interstitial carbon atoms in Pd is well documented. Exposure of Pd to C₂H₄, C₂H₂, and CO at 423–773 K produced C/Pd ratios up to 0.15, increased the Pd lattice constant to 0.399 nm, and simultaneously decreased the hydride-forming ability until no hydride was formed in PdC_{0.15} (34, 68). Ziemecki *et al.* showed that the carbon was located in Pd octahedral sites (68–70). Interstitial carbon was also indicated by a 2.8% expansion of the Pd lattice when Pd films were deposited by vacuum evaporation on a cooled carbon substrate (71). An *in situ* EXAFS study of Pd/C and Pd/Al₂O₃ catalysts by McCaulley showed the presence of interstitial carbon after exposure to C₂H₄, accompanied by lattice expansion and suppression of hydride formation (72). Although a lattice expansion of 3% has been proposed for 1–2 nm Pd particles with an incompletely developed fcc structure (73), this possibility is inapplicable here because the Pd crystallites are larger in our catalysts.

Ziemecki *et al.* observed the decomposition of the bulk PdC_x phase at 873 K in an inert atmosphere and at 423 K in H₂ or O₂ (68), while Stachurski observed it at 610 K in an Ar atmosphere or under vacuum and at 460 K in H₂ (29). Lamber *et al.* saw this decomposition in 2–5 nm Pd particles supported on amorphous carbon at 700 K under vacuum, accompanied by carbon deposition on the Pd surface (71). Recently, Yamamoto *et al.* have synthesized 5-nm Pd carbide particles by vapor condensation in acetone vapor and this Pd carbide phase converts to metallic Pd above 673 K (74). Maciejewski and Baiker prepared 5–7 nm PdC_x crystallites on ZrO₂ using CO; the PdC_x phase remained stable to 670 K but decomposition to elemental Pd and C occurred at higher temperatures (75).

LEED studies of a Pd(110) surface by Wolf *et al.* showed that carbon segregates to the surface at 400–600 K (76). After reactive cleaning cycles with O₂ at 640 K or heating the crystal to above 1000 K, the carbon reappeared on the Pd surface during cooling, and carbon at or near the Pd surface increased the average interlayer spacing of the first 3–4 interplanar spacings by about 4% (76). Hamilton and Blakely reported an abrupt transition from a clean Pd (100) or (111) surface to one covered with a monolayer of carbon as the temperature decreased, and a graphitic surface precipitate occurred between 928 and 1168 K (77). The temperature dependence of carbon segregation on Pd(111) surfaces, studied by CO desorption spectra, showed that carbon does not segregate to the surface at temperatures <835 K during heating under vacuum, and the temperature range in which C atoms remain segregated at the surface depends on the C/Pd ratio (78).

These studies establish that Pd–C phases can exist, although single-crystal results imply that little or no interstitial bulk carbon would be expected in the current Pd/C catalysts due to the low solubility of C in Pd in the temperature range 298 to 673 K. However, the lattice expansion

seen by XRD in the current study indicates that interstitial C is present in these small Pd crystallites after reduction and evacuation at 573 K, and the formation of this PdC_x phase may be facilitated in small Pd crystallites in direct contact with carbon (29, 69, 71, 77). In these Pd/C catalysts, Pd particles are located in the small pores of a turbostratic carbon thus enhancing Pd–C contact, and the possibility of an interaction between Pd and carbon at the Pd–C interface has been suggested by the theoretical calculations of Baetzold (79). Such an interaction could weaken C–C bonds and facilitate the formation of a solid solution both at the Pd–C interface and in the bulk, as suggested for highly dispersed Ni, Pd, and Pt on amorphous carbon during its catalyzed conversion to graphitic carbon (80–84). The mechanism proposed for the Pd catalyzed gasification of amorphous carbon involves the breaking of C–C bonds at the Pd–C interface, diffusion of C into the Pd, precipitation of C atoms as graphite on the Pd surface at high temperatures, and finally reaction of dissociatively adsorbed gases with these C atoms to form gas-phase products like CH₄ or CO₂ (82). The free energy difference between the initial disordered carbon and the final graphitic form of carbon is thought to be the driving force for this mechanism; hence, this sequence may not occur on graphitic carbon (80). Complete encapsulation and partial coverage of Ni and Pd particles on amorphous carbon has been observed using HRTEM (71, 81).

In the present study it can be suggested that the source of the carbon on and in the Pd crystallites is from either the Pd(AcAc)₂ precursor or the solvent (THF). The latter possibility is discounted because similar preparation techniques using THF have been used previously to prepare Fe, Ru, Os, and Co supported on a similar carbon black (85–87), and no contamination by carbon was observed. In regard to Pd(AcAc)₂, however, it is less clear although evidence exists that argues against it being the carbon source. First, it decomposes at 478 K (88). Second, Pd/La₂O₃ catalysts made from Pd(AcAc)₂ had higher dispersions after decomposition in He compared to those after calcination in air prior to reduction, thus indicating no C contamination (33). Third, the formation of clean, highly dispersed Pt clusters on KL zeolites was obtained by the decomposition of Pt hexafluoroacetylacetonate under H₂ at 623 K (89, 90). An analogous decomposition mechanism has been suggested for Pd(AcAc)₂, where release of acetylacetonate was observed during contact of Pd(AcAc)₂ with alumina (18). Finally, Pd/Al₂O₃ catalysts prepared from Pd(AcAc)₂ produced highly dispersed Pd particles (<1 nm) which stoichiometrically adsorbed CO after calcination in air followed by reduction under H₂, both at 573 K (18), thus indicating that our treatment in O₂ at 573 K prior to reduction should have produced clean Pd surfaces. However, chemisorption remained suppressed after such treatments in O₂; furthermore, the decrease

in CO uptakes after sequential O₂ treatments (following reduction) suggests that the contamination occurs during the reduction step or, more likely, the evacuation step at 573 K (20). Regardless, the possibility that decomposition of Pd(AcAc)₂ in these small pores may leave residual C atoms cannot be entirely dismissed.

Another indication that Pd(AcAc)₂ is not the only source of the carbon contaminant in these Pd/C catalysts is that the suppression of hydrogen chemisorption has also been observed for Pd dispersed on turbostratic carbons using H₂PdCl₄ or Pd(NH₃)₄(NO₃)₂ as precursors (16, 20), but such a suppression was not seen when Pd(NH₃)₄(NO₃)₂ was reduced on Grafoil, as shown in Table 3 and elsewhere (20). The suppressed chemisorption and hydride formation was not accompanied by lattice expansion in the catalysts made from H₂PdCl₄. However, a higher hydride ratio of 0.53 for a 7.1% Pd/C catalyst made from H₂PdCl₄ after reduction at 523 K decreased to 0.43 after reduction at 573 K, indicating that contamination of the Pd surface in these systems may be dependent on the reduction or evacuation temperature (20).

The previous discussion suggests that when Pd is in contact with a clean, highly disordered carbon surface, such as this turbostratic carbon black, it may be more facile for carbon to migrate onto and into the Pd crystallites during the higher temperature reduction or evacuation periods. The dissolution of C from an activated carbon support into the bulk of Ni crystallites, as well as C precipitation on the Ni surface during thermal treatments in N₂ or Ar or H₂ activation above 723 K, has been proposed recently to explain decreased catalytic activity of Ni for acetone hydrogenation (91). The dissolution and diffusion of carbon species through the bulk of metals is considered a key step in the formation of carbon filaments from hydrocarbon reactions over metal surfaces (92). The preparation technique used here will disperse the Pd particles in the small pores of the carbon, thus enhancing the Pd–C interface.

Based on the previous discussion, five types of Pd particles can be proposed to coexist in these Pd/C catalysts, as shown in Fig. 6: Type A, clean Pd particles, free of both bulk and surface carbon impurities, exhibiting normal chemisorption and hydride formation; Type B, Pd particles completely encapsulated by carbon and incapable of either adsorbing gas or forming a hydride; Type C, Pd particles partially covered by carbon as well as having interstitial carbon, exhibiting both suppressed chemisorption and hydride formation; Type D, Pd particles partially covered by carbon but with no interstitial carbon, which show suppressed chemisorption but normal hydride behavior; and Type E, Pd particles with clean surfaces but with interstitial carbon, resulting in normal chemisorption but suppressed hydride formation. Type E particles can be eliminated based on the thermodynamics of surface segregation of carbon in Pd, since carbon on the Pd surface is necessary

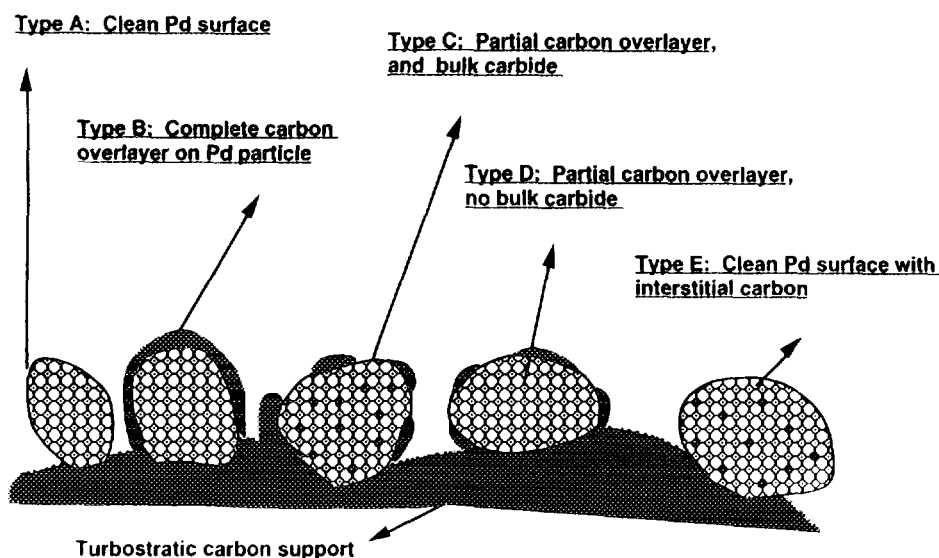


FIG. 6. Pd particles that may form on a high surface area carbon.

to stabilize carbon in the bulk (76, 77); this requirement is supported by our results showing that suppression of β -hydride formation was always accompanied by suppressed chemisorption in these Pd/C catalysts.

Two limiting models can be proposed as the simplest explanations of the behavior of these Pd/C catalysts. One (Model I) invokes a mixture of Pd particles with no interstitial carbon but with extremely different extents of surface contamination—either clean or completely encapsulated Pd particles, i.e., Type A and B particles. Thus, in this extreme case, the Pd particles can both chemisorb and form hydride or they cannot do either. This model can qualitatively explain both the suppression of chemisorption and hydride formation, but it does not predict the observed bulk hydride ratio (20) and, in addition, it cannot explain the expansion of the Pd lattice seen by XRD. Calculations for determining the consistency of this model were made assuming the existence of uniform, spherical particles with a diameter corresponding to the surface-area-average diameter, d_s , from TEM; Model I inferred that 80–90% of the Pd crystallites were completely encapsulated, it always predicted bulk hydride ratios 2–5 times lower than observed, and it could not explain the high $\text{CO}_{\text{ad}}/\text{H}_{\text{ad}}$ ratios (20). This, coupled with its inability to explain the lattice expansion, forced its dismissal.

Consequently, the simplest model to explain the phenomena observed in this study is the proposal that Pd particles exist with both bulk and surface carbon contamination, i.e., all are Type C particles (Model II). The extent of the Pd surface covered by carbon according to Model II was again calculated using d_s and the amount of chemisorbed hydrogen or CO (assumed to count Pd_s atoms) and the results are in Table 6. The observed β -hydride ratios are

given in column 3, while the apparent $\text{C}_{\text{bulk}}/\text{Pd}_{\text{bulk}}$ ratios, assuming an $\text{H}_{\text{ab}}/\text{Pd}_{\text{bulk}}$ ratio of 0.66 and that one interstitial C atom blocks four such sites for H atoms (34), are listed in column 4. The $\text{C}_{\text{bulk}}/\text{Pd}_{\text{bulk}}$ ratios of 0.05–0.10 in these Pd/C catalysts are presumably stabilized at 298 K by the presence of carbon on the surface of these Pd particles (76, 77). The ratios of $\text{CO}_{\text{ad}}/\text{H}_{\text{ad}}$ in column 5, which are higher than the expected ratio near unity, can now be rationalized by this model. The larger uptakes of CO compared to H_2 and O_2 are consistent with the fact that H_2 and O_2 need two adjacent three- or fourfold hollow sites for dissociation, the population of which would decrease more rapidly than on-top sites due to occupancy of these hollow sites by C atoms, whereas CO could still adsorb linearly on single (on-top) sites. Thus the carbon coverage of the Pd surface calculated on the basis of CO chemisorption, shown in Table 6, is lower than that based on H_2 chemisorption; however, the actual coverage of the Pd surface by carbon may well be between these two values.

The values of heats of adsorption of H_2 and CO are consistent with the above model of partial coverage of surface Pd atoms. Both H_2 and CO chemisorption on clean Pd surfaces increase the work function; however, the maximum increase is about four times greater with CO (93, 94). Q_{ad} values for H_2 relate more closely to the initial Q_{ad} values 20 to 27 kcal/mole than to the integral Q_{ad} values 15 ± 1 kcal/mole, as shown in Table 5 (15, 40–48). The somewhat higher Q_{ad} values for H_2 , compared to Pd/oxide catalysts, indicate that the remaining hollow sites on the Pd that are capable of adsorbing H atoms retain a strong bond comparable to that on clean Pd single-crystal surfaces (15, 40). The Q_{ad} values for H_2 are consistent with the low surface coverages of H atoms that exist on these catalysts,

TABLE 6
Extent of Surface Coverage by Carbon and Bulk Carbide Formation for C-Supported Pd
Based on Model II

Catalyst	Fraction of Pd surface covered by C		Observed H_{ab}/Pd_{bulk} <i>c</i>	Calculated C_{bulk}/Pd_{bulk} <i>d</i>	(CO_{ad}/H_{ad})	Maximum monolayer after bulk C migration to Pd surface	
	<i>a</i>	<i>b</i>				<i>f</i>	<i>g</i>
2.6% Pd/C-AS IS	0.80	0.77	0.37	0.07	1.1	0.97	0.94
2.8% Pd/C-HTT-H ₂	0.87	0.43	0.27	0.10	4.4	1.19	0.75
2.8% Pd/C-HTT-H ₂ ^e	0.55	0.43	0.44	0.05	1.3	0.71	0.59
3.1% Pd/C-HTT-Ar	0.79	0.52	0.25	0.10	2.3	1.19	0.92
2.3% Pd/C-HNO ₃	0.88	0.82	0.41	0.06	1.5	1.20	1.14
2.3% Pd/C-HNO ₃ ^e	0.76	0.62	0.48	0.05	1.6	1.03	0.89

^a Based on chemisorbed H₂.

^b Based on chemisorbed CO.

^c Based on dispersion from TEM.

^d Assuming 1 C atom blocks 4 interstitial sites for H (Ref. 34).

^e Heated in 2% O₂ for 30 min at 573 K before reduction.

^f Based on ^a.

^g Based on ^b.

thus mimicking the higher initial values on single Pd crystals. The Q_{ad} values for H₂ for these Pd/C catalysts are similar to values obtained for PdCu(111), where the number of Pd triplet sites decreased due to the presence of Cu (95). In contrast, the Q_{ad} values for CO are somewhat lower than those found for dispersed Pd crystallites (52). These lower values are consistent with the observed decrease in CO adsorption on high-energy sites on a carbon-covered Pd surface; in addition, the Q_{ad} of CO on these higher energy sites was lowered, resulting in a net decrease in the heat of CO adsorption (53). The lower Q_{ad} values for CO may thus be a consequence of CO adsorption only on singlet (on-top) sites of lower energy. Such lower CO heats of adsorption were also obtained for PdCu(111) and PdAg(111) surfaces due to a decrease in CO adsorption on triplet sites (95, 96). It is also possible that the latter Q_{ad} values may also reflect a substantial amount of CO dissociation, as found previously for CO adsorption on Fe/C catalysts (97), as well as Pd catalysts (53).

Model II can explain the chemisorption behavior of these Pd/C catalysts in the following way. Reducing conditions above 673 K cause a shrinkage of the Pd lattice, as indicated by XRD, and provide normal hydride formation, but chemisorption is still suppressed, as shown in Tables 2 and 4. At these higher temperatures bulk carbon atoms diffuse to the Pd surface and the maximum coverage of the Pd surface if all the carbon from the bulk migrated to the surface is 0.6–1.2 monolayers, which explains the continued suppression of chemisorption after this pretreat-

ment. Although some sintering is associated with higher reduction temperatures (Table 4), the particle sizes from chemisorption are much larger than that from XRD, showing that substantial suppression of chemisorption still exists. Hence, carbon remains on the Pd surface after evacuation and cooling following reduction. This model is also consistent with the effects of an O₂ regeneration step: the evolution of CO and CO₂, the contraction of the Pd lattice, and the increase in both the hydride ratio and H₂ and O₂ uptakes, as shown in Tables 2 and 4. After the O₂ treatment the CO uptake was more consistent with the H₂ and O₂ uptakes; however, this sequence of mild cleaning in O₂ followed by reduction in H₂ and evacuation at 573 K did not remove all the carbon. Three possibilities could account for this behavior: (1) Diffusional limitations may exist for interstitial C atoms to migrate to the surface and react with oxygen (98); (2) completely encapsulated Pd particles would not be able to adsorb and dissociate O₂ at 573 K (82, 83); or (3) C atoms may migrate from the support to the Pd during the reduction/evacuation step in H₂ at 573 K following the O₂ pretreatment. At this time the last explanation is favored.

Consequently, Model II, which assumes the presence of Type C particles only, is the simplest one to explain all the observed phenomena, but the simultaneous presence of Type A, B, and D particles (Fig. 6) cannot be ruled out; however, Type C particles *must* be present. The Pd surface can also be contaminated by sulfur from the carbon support in the Pd/C-AS IS sample. This model also explains the

absence of chemisorption and anomalous calorimetric results reported by Phillips and co-workers and eliminates their need to postulate that H₂ does not chemisorb on bulk or carbon-supported Pd at 300 K (16), a premise disproven by all other studies (7, 9, 24, 38–42, 45, 93, 95, 96, 99–102). Their results were further complicated by the absence of a cleaning procedure in O₂ and the fact that their Monarch 700 carbon support can contain as much as 1.3 wt% S (103), as either factor can also suppress chemisorption. These considerations and others are discussed in greater detail elsewhere (20).

SUMMARY

The pretreatment of a turbostratic carbon support prior to its impregnation with Pd(AcAc)₂ under anaerobic conditions had little effect on the Pd dispersion although a nitric acid treatment to add oxygen-functional groups on the surface decreased the Pd dispersion slightly. Chemisorption of H₂, O₂, and CO was suppressed on the Pd crystallites dispersed on these clean carbon supports, which is due to contamination of the Pd surface by carbon. Additional contamination of Pd by sulfur impurities in the carbon can occur if the sulfur is not removed. Suppressed chemisorption, low bulk β-hydride ratios, an expanded Pd lattice after pretreatment and evacuation, and high CO_{ad}/H_{ad} ratios are all indicative of contamination by C atoms and the formation of a bulk PdC_x phase. A model invoking partial coverage of the Pd surface by carbon atoms along with carbon atoms occupying interstitial positions in the Pd lattice can explain the above characteristics. Thus carbon atoms from either the acetylacetonate group or the turbostratic carbon support appear to migrate onto and into Pd crystallites dispersed within the carbon black pore structure during the period of H₂ reduction and evacuation at 573 K. Exposure to reducing conditions above 673 K causes the carbon in the interstitial sites to migrate to the surface and give XRD patterns indicative of pure Pd. A treatment in O₂ at 573 K can remove the carbon from the Pd, but the carbon appears to reestablish itself during the subsequent reduction/evacuation step.

ACKNOWLEDGMENTS

This study was funded by the National Science Foundation under Grant CTS-9011275. We thank Kevin Appold for conducting some of the O₂ pretreatment studies during a summer REU program sponsored by the NSF.

REFERENCES

- Jungten, H., *Fuel* **65**, 1436 (1986).
- Bird, A. J., in "Catalyst Supports and Supported Catalysts" (A. B. Stiles, Ed.), p. 107. Butterworth, Stoneham, MA, 1987.
- Cameron, D. S., Cooper, S. J., Dodgson, I. L., Harrison, B., and Jenkins, J. W., *Catal. Today* **7**, 113 (1990).
- Albers, P., Deller, K., Despeyroux, B. M., Schafer, A., and Seibold, K., *J. Catal.* **133**, 467 (1992).
- Heal, G. R., and Mkyula, L. L., *Carbon* **26**, 803 (1988).
- Leon Y., Leon, C. A., and Radovic, L. R., *ACS Preprints Div. Fuel Chem. NY* p. 1007 (1991).
- Suh, D. J., Park, T. J., and Ihm, S. K., *Carbon* **31**, 427 (1993).
- Chou, P., and Vannice, M. A., *J. Catal.* **107**, 129 (1987).
- Ouchaib, T., Moraweck, B., Massardier, J., and Renouprez, A., *Catal. Today* **7**, 191 (1990).
- Krishnankutty, N., and Vannice, M. A., *J. Catal.* **155**, 327 (1995).
- Krishnankutty, N., and Vannice, M. A., *Chem. Mater.*, **7**, 754 (1995).
- Bansal, R. C., Vastola, F. J., and Walker, P. L., Jr., *J. Colloid Interface Sci.* **32**, 187 (1970).
- Puri, B. R., *Chem. Phys. Carbon* **6**, 191 (1970).
- Shriver, D. F., "The Manipulation of Air-Sensitive Compounds." McGraw Hill, New York, 1969.
- Chou, P., and Vannice, M. A., *J. Catal.* **104**, 1 (1987).
- Wunder, R. W., Cobes, J. W., Phillips, J., Radovic, L. R., Lopez Peinado, A. J., and Carrasco-Marin, F., *Langmuir* **9**, 984 (1993).
- Seyedmonir, S. R., Strohmayer, D. E., Geoffroy, G. L., and Vannice, M. A., *Adsorpt. Sci. Technol.* **1**, 253 (1984).
- Boitiaux, J. P., Cosyns, J., and Vasudevan, S., "Preparation of Catalysts III" (G. Poncelet, P. Grange and P. A. Jacobs, Eds.) p. 123. Elsevier, Amsterdam, 1983.
- Ryndin, Yu. A., Stenin, M. V., Boronin, A. I., Bukhtiyarov, V. I., and Zaikovskii, V. I., *Appl. Catal.* **54**, 277 (1989).
- Krishnankutty, N., Ph.D. thesis, The Pennsylvania State University, May, 1994.
- Benson, J. E., Hwang, H. S., and Boudart, M., *J. Catal.* **30**, 146 (1973).
- Yates, D. J. C., and Sinfelt, J., *J. Catal.* **8**, 348 (1967).
- Vannice, M. A., Sen, B., and Chou, P., *Rev. Sci. Instrum.* **58**, 647 (1987).
- Martin, N., and Fuentes, S., *Carbon* **26**, 795 (1988).
- Gubitosa, G., Berton, A., Camia, M., and Pernicone, N., "Preparation of Catalysts III" (G. Poncelet, P. Grange, and P. A. Jacobs, Eds.) p. 431. Elsevier, Amsterdam, 1983.
- Pope, D., Smith, W. L., Eastlake, M. J., and Moss, R. I., *J. Catal.* **22**, 72 (1971).
- Heinemann, K., Osaka, T., Poppa, H., and Avalos-Borja, M., *J. Catal.* **83**, 61 (1983).
- Palczewska, W., *Adv. Catal.* **24**, 245 (1975).
- Stachurski, J., *J. Chem. Soc. Faraday Trans. 1* **81**, 2813 (1985).
- Aben, P. C., *J. Catal.* **10**, 224 (1968).
- Leon y Leon, C. A., and Vannice, M. A., *Appl. Catal.* **69**, 269 (1991).
- Hicks, R. F., Yen, Q.-J., and Bell, A. T., *J. Catal.* **89**, 498 (1984).
- Sudhakar, C., and Vannice, M. A., *Appl. Catal.* **14**, 47 (1985).
- Ziemecki, S. B., Michel, J. B., and Jones, G. A., *React. Solids* **2**, 187 (1987).
- Boudart, M., and Hwang, H. S., *J. Catal.* **39**, 44 (1975).
- Bonivardi, A. L., and Baltanas, M. A., *J. Catal.* **138**, 500 (1992).
- Jobic, H., and Renouprez, A., *J. Less-Common Met.* **129**, 311 (1987).
- Konvalinka, J. A., and Scholten, J. J. F., *J. Catal.* **48**, 374 (1977).
- Gentsch, H., Guillen, N., and Köpp, M., *Z. Phys. Chem. N. F.* **82**, 49 (1972).
- Conrad, H., Ertl, G., and Latta, E. E., *Surf. Sci.* **41**, 435 (1974).
- Behm, R. J., Christmann, K., Ertl, G., *Surf. Sci.* **99**, 320 (1980).
- Aldag, A. W., and Schmidt, L. D., *J. Catal.* **22**, 260 (1971).
- Zakumbaeva, G. D., Zakarina, N. A., Naidin, V. A., Dostiyarov, A. M., Toktabaeva, N. F., and Litvyakova, E. N., *Kinet. Catal.* **24**, 379 (1983).
- Vert *et al.*, *Dokl. Akad. Nauk SSSR* **140**, 149 (1961).
- Beck, O., *Discuss Faraday Soc.* **8**, 118 (1950).
- Leary, K. J., Michaels, J. N., and Stacy, A. M., *Langmuir* **4**, 1251 (1988).

47. Watanabe, M., Wedler, G., Wissmann, P., *Surf. Sci.* **154**, L207 (1985).
48. Gravelle-Rumeau-Maillot, M., Pitchon, V., Martin, G. A., and Prali-aud, H., *Appl. Catal. A* **98**, 45 (1993).
49. Chou, P., and Vannice, M. A., *J. Catal.* **105**, 342 (1987).
50. Vannice, M. A., and Chou, P., in "Strong Metal-Support Interac-tions", (R. T. K. Baker, S. J. Tauster, and J. A. Dumesic, Eds.), ACS Symposium Series, p. 76 Am. Chem. Soc., Washington, DC, 1986.
51. Henry, C. R., Chapon, C., Goyhenex, C., and Monot, P., *Surf. Sci.* **272**, 283 (1992).
52. Chou, P., and Vannice, M. A., *J. Catal.* **104**, 17 (1987).
53. Stará, I., Matolín, V., *Surf. Sci.* **313**, 99 (1994).
54. Paseka, I., *Collect. Czech. Chem. Commun.* **57**, 1793 (1992).
55. Nace, D. M., and Aston, J. G., *J. Am. Chem. Soc.* **79**, 3619 (1957).
56. Picard, C., Kleppa, O. J., and Boureau, G., *J. Chem. Phys.* **69**, 5549 (1978).
57. Kuji, T., Oates, W. A., Bowerman, B. S., and Flanagan, T. B., *J. Phys. F* **13**, 1785 (1983).
58. Flanagan, T. B., and Lynch, J. F., *J. Phys. Chem.* **79**, 444 (1975).
59. Foo, C. H., Hong, C. T., Yeh, C. T., *J. Chem. Soc. Farad. Trans. 1* **85**, 65 (1989).
60. Kishimoto, S., Inoue, M., Yoshida, N., and Flanagan, T. B., *J. Chem. Soc. Farad. Trans.* **82**, 2175 (1986).
61. Artamonov, S. V., Zakumbaeva, G. D., Soklo'skii, D. V., *Dokl. Akad. Nauk SSSR* **244**, 123 (1979).
62. O'Rear, D. J., Löffler, D. G., and Boudart, M., *J. Catal.* **94**, 225 (1985).
63. Solymosi, F., and Kovacs, I., *Surf. Sci.* **260**, 139 (1992).
64. Barbier, J., Lamy-Pitara, E., Marcelot, P., Boitiaux, J. P., Cosyns, J., and Verna, F., *Adv. Catal.* **37**, 279 (1990).
65. Frieske, H., and Wicke, E., *Ber. Bunsen-Ges.* **48** (1972).
66. Chen, A., Benesi, A., and Vannice, M. A., *J. Catal.* **119**, 14 (1989).
67. Toth, L. E., "Transition Metal Carbides and Nitrides," p. 2. Aca-demic Press, New York, 1971.
68. Ziemecki, S. B., Jones, G. A., Swartzfager, D. G., and Harlow, R. L., *J. Am. Chem. Soc.* **107**, 4547 (1985).
69. Ziemecki, S. B., and Jones, G. A., *J. Catal.* **95**, 621 (1985).
70. Ziemecki, S. B., Jones, G. A., and Swartzfager, D. G., *J. Less-Common Met.* **131**, 157 (1987).
71. Lamber, R., Jaeger, N., and Schulz-Ekloff, G., *Surf. Sci.* **227**, 15 (1990).
72. McCaulley, J. A., *J. Phys. Chem.* **97**, 10372 (1993).
73. Heinemann, K., and Poppa, H., *Surf. Sci.* **156**, 265 (1985).
74. Yamamoto, T., *et al.*, *Appl. Phys. Lett.* **63**, 3020 (1993).
75. Maciejewski, M., and Baiker, A., *J. Phys. Chem.* **98**, 285 (1994).
76. Wolf, M., Goschnick, A., Loboda-Cackovic, J., Grunze, M., Unertl, W. N., and Block, J. H., *Surf. Sci.* **182**, 489 (1987).
77. Hamilton, J. C., and Blakely, J. M., *Surf. Sci.* **91**, 199 (1980).
78. Ratajczykowa, I., *J. Vac. Sci. Technol. A* **1**, 1512 (1983).
79. Baetzold, R. C., *Surf. Sci.* **36**, 123 (1972).
80. Holstein, W. L., Moorhead, R. D., Poppa, H., and Boudart, M., *Chem. Phys. Carbon* **18**, 139 (1982).
81. Lamber, R., Jaeger, N., and Schulz-Ekloff, G., *Surf. Sci.* **197**, 402 (1988).
82. Boudart, M., Holstein, W. L., Moorhead, R. D., and Poppa, H., *Appl. Catal.* **11**, 117 (1984).
83. Su, H.-I., Heinemann, K., Poppa, H., and Boudart, M., *J. Solid State Chem.* **106**, 55 (1993).
84. Lamber, R., and Jaeger, N. I., *Surf. Sci.* **289**, 247 (1993).
85. Venter, J. J., Ph.D. thesis, The Pennsylvania State University, 1989.
86. Venter, J., Kaminsky, M., Geoffroy, G. L., and Vannice, M. A., "Preparation of Catalysts IV" (B. Delmon, P. Grange, P. A. Jacobs, and G. Poncelet, Eds.), p. 479. Elsevier, Amsterdam, 1987.
87. Chen, A., Kaminsky, M., Geoffroy, G. L., and Vannice, M. A., *J. Phys. Chem.* **90**, 4810 (1986).
88. Aldrich Chemical Co., private communication.
89. Dossi, C., Psaro, R., Bartsch, A., Fusi, A., Sordelli, L., Ugo, R., Bellatreccia, M., Zanoni, R., and Vlačić, G., *J. Catal.* **145**, 377 (1984).
90. Dossi, C., Psaro, R., Bartsch, A., Brivio, E., Galasco, A., and Losi, P., *Catal. Today* **17**, 527 (1993).
91. Gandia, L. M., and Montes, M., *J. Catal.* **145**, 276 (1994).
92. Baker, R. T. K., Barber, M. A., Harris, P. S., Feates, F. S., and Waite, R. J., *J. Catal.* **26**, 51 (1972).
93. Cattania, M. G., Penka, V., Behm, R. J., Christmann, K., and Ertl, G., *Surf. Sci.* **126**, 382 (1986).
94. Ertl, G., and Koch, J., in "Adsorption-Desorption Phenomena, Pro-ceedings of the Second International Conference" (F. Ricca, Ed.) p. 345, Academic Press, New York, 1972.
95. Noordermeer, A., Kok, G. A., and Nieuwenhuys, B. E., *Surf. Sci.* **172**, 349 (1986).
96. Noordermeer, A., Kok, G. A., and Nieuwenhuys, B. E., *Surf. Sci.* **165**, 375 (1986).
97. Venter, J. J., Chen, A. A., Phillips, J., and Vannice, M. A., *J. Catal.* **119**, 45 (1989).
98. Zaidi, A. H., *Appl. Catal.* **30**, 131 (1987).
99. Polyanszky, É., and Petró, J., *Appl. Catal.* **62**, 335 (1990).
100. Everett, D. H., and Sermon, P. A., *Z. Phys. Chem. NF* **114**, 101 (1979).
101. He, J.-W., and Norton, P. R., *Surf. Sci.* **195**, L199 (1988).
102. Ragaini, V., Giannantonio, R., Magni, P., Lucarelli, L., and Leofanti, G., *J. Catal.* **146**, 116 (1994).
103. Mulay, L. N., Prasad Rao, A. V., Rivera-Utrilla, J., Walker, P. L., Jr., and Vannice, M. A., *Carbon* **23**, 493 (1985).